Tautomeric states of the active-site histidines of phosphorylated and unphosphorylated III^{Glc}, a signal-transducing protein from *Escherichia coli*, using two-dimensional heteronuclear NMR techniques

J.G. PELTON,[1] D.A. TORCHIA,[1] N.D. MEADOW,[2] AND S. ROSEMAN[2]

[1] Bone Research Branch, National Institute of Dental Research, National Institutes of Health, Bethesda, Maryland 20892
[2] Department of Biology and McCollum-Pratt Institute, The Johns Hopkins University, Baltimore, Maryland 21218

Abstract

III^{Glc} is an 18.1-kDa signal-transducing phosphocarrier protein of the phosphoenolpyruvate:glycose phosphotransferase system from *Escherichia coli*. The ^{1}H, ^{15}N, and ^{13}C histidine ring NMR signals of both the phosphorylated and unphosphorylated forms of III^{Glc} have been assigned using two-dimensional ^{1}H-^{15}N and ^{1}H-^{13}C heteronuclear multiple-quantum coherence (HMQC) experiments and a two-dimensional ^{13}C-^{13}C-^{1}H correlation spectroscopy via J$_{CC}$ coupling experiment. The data were acquired on uniformly ^{15}N-labeled and uniformly ^{15}N/^{13}C-labeled protein samples. The experiments rely on one-bond and two-bond J couplings that allowed for assignment of the signals without the need for the analysis of through-space (nuclear Overhauser effect spectroscopy) correlations. The ^{15}N and ^{13}C chemical shifts were used to determine that His-75 exists predominantly in the N$^{\varepsilon 2}$-H tautomeric state in both the phosphorylated and unphosphorylated forms of III^{Glc}, and that His-90 exists primarily in the N$^{\delta 1}$-H state in the unphosphorylated protein. Upon phosphorylation of the N$^{\varepsilon 2}$ nitrogen of His-90, the N$^{\delta 1}$ nitrogen remains protonated, resulting in the formation of a charged phospho-His-90 moiety. The ^{1}H, ^{15}N, and ^{13}C signals of the phosphorylated and unphosphorylated proteins showed only minor shifts in the pH range from 6.0 to 9.0. These data indicate that the pK_a values for both His-75 and His-90 in III^{Glc} and His-75 in phospho-III^{Glc} are less than 5.0, and that the pK_a value for phospho-His-90 is greater than 10. The results are presented in relation to previously obtained structural data on III^{Glc}, and implications for proposed mechanisms of phosphoryl transfer are discussed.

Keywords: histidine tautomer; low histidine pK_a; phosphoenolpyruvate phosphotransferase system; phosphohistidine

The phosphoenolpyruvate:glycose phosphotransferase system is responsible for the uptake and concomitant phosphorylation of its sugar substrates in preparation for their catabolism by the cell. This system also regulates the uptake of non-PTS sugars in response to changing environmental conditions leading to the phenomenon of diauxie. The 18.1-kDa phosphocarrier protein III^{Glc}, which is encoded by the *crr* gene, was found to be essential for proper PTS function. III^{Glc} plays a central role in both the transport and regulatory functions of the PTS. In glucose transport a phosphoryl group derived from PEP is transferred to III^{Glc} via the proteins Enzyme I and HPr. A complex between phospho-III^{Glc} (P-III^{Glc}) and the membrane-associated protein EIIB^{Glc} is then responsible for glucose phosphorylation and translocation.

The regulatory role of III^{Glc} is governed by its extent of phosphorylation; in this capacity the protein is thought to effect the modulation of the activity of the melibiose, lactose, and maltose permeases, as well as adenylate cyclase, and glycerol kinase. For reviews see Postma and Lengeler (1985), Saier (1989), Meadow et al. (1990), and Roseman and Meadow (1990).

Of the PTS proteins, the structure of HPr has been the most intensively studied and continues to be a subject of active research (Klevit & Waygood, 1986; El Kabbani et al., 1987; Hammen et al., 1991; Sharma et al., 1991; Herzberg et al., 1992; van Nuland et al., 1992; Wittekind et al., 1992). More recently, NMR and X-ray structural studies of III^{Glc} from *Escherichia coli* (Pelton et al., 1991a,b, 1992; Worthylake et al., 1991) and the IIA domain of the *Bacillus subtilis* glucose permease (Fairbrother et al., 1991a,b, 1992; Liao et al., 1991) have been completed. These proteins have 42% sequence identity and have similar although not identical structures (Worthylake et al., 1991). In both proteins the heart of the active site consists of a pair of histidine residues (His-75 and His-90 in *E. coli*) that are conserved in a large number of sugar-specific PTS proteins and non-PTS permeases (Meadow et al., 1990; Liao et al., 1991). Biochemical studies have shown that the N$^{\epsilon 2}$ nitrogen of His-90 is phosphorylated (Meadow & Roseman, 1982; Dörschug et al., 1984). In addition, studies of mutant proteins indicate that both histidines are required for complete phosphocarrier and regulatory activity (Presper et al., 1989). Moreover, mechanisms for phosphoryl transfer have been proposed on the basis of the activity of the mutant proteins (Presper et al., 1989), and the X-ray-derived model of the IIA domain from *B. subtilis* (Liao et al., 1991). To date, however, the protonation states of the histidines in III^{Glc} and the IIA domain, knowledge of which is central to elucidation of the mechanism of phosphoryl transfer, remain unknown despite speculation on the basis of hydrogen-bonding considerations (Liao et al., 1991; Worthylake et al., 1991).

NMR spectroscopy is ideally suited to the study of the protonation states of histidine residues in proteins (for a review see Markley [1975]). In particular, the development of ^{15}N and ^{13}C heteronuclear methods have increased the molecular weight range accessible to this technique (Fesik & Zuiderweg, 1990; Wang et al., 1990; Clore & Gronenborn, 1991; Grzesiek & Bax, 1992) and, more importantly to the present study, can provide information on the predominant tautomeric state of a histidine residue (Reynolds et al., 1973; Bachovchin & Roberts, 1978). Recent examples include studies of the tautomeric states of the active-site histidines of α-lytic protease (Bachovchin, 1986), triosephosphate isomerase (Lodi & Knowles, 1991), HPr (van Dijk et al., 1990), *E. coli* Enzyme-IIA^{mtl} (van Dijk et al., 1992), and *E. coli* β-hydroxydecanoyl thiolester dehydrase (Annand et al., 1992). In order to better understand the role of the active-site histidines of *E.*

coli III^{Glc} in phosphoryl transfer, we have assigned the imidazole ^{1}H, ^{15}N, and ^{13}C signals of His-75 and His-90 for both III^{Glc} and P-III^{Glc} using 2D heteronuclear techniques. From these data we have determined the predominant tautomeric state of each of these histidines in both forms of the protein.

Results

Identification of histidine imidazole ^{1}H and ^{13}C spin systems

In the aromatic region of the ^{1}H spectrum of III^{Glc}, signals from His-75 and His-90 as well as those from the eight phenylalanine residues are present. Early results on amino acids (Reynolds et al., 1973; Howarth & Lilley, 1978) and short peptides (Richarz & Wüthrich, 1978) conducted at various pH values showed that the histidine signals could be distinguished from those of phenylalanine on the basis of ^{13}C chemical shifts and both $^1J_{CH}$ and $^1J_{CC}$ coupling constants (Bystrov, 1976). Typically, histidine ^{13}C$^{\epsilon 1}$ signals (ca. 140 ppm) resonate ca. 10 ppm downfield of ^{13}C$^\delta$, ^{13}C$^\epsilon$, and ^{13}C$^\zeta$ phenylalanine signals (ca. 130 ppm), whereas histidine ^{13}C$^{\delta 2}$ signals resonate near to or upfield of these phenylalanine aromatic resonances depending on the protonation state of the ring (Reynolds et al., 1973). ^{13}C NMR studies also showed that histidine ring $^1J_{CH}$ coupling constants (e.g., $^1J_{C^{\epsilon 1}H^{\epsilon 1}}$, 208–222 Hz) (Bystrov, 1976), although a function of pH, are substantially larger than for those of the phenylalanine ring (ca. 155 Hz). In addition, the histidine C$^\gamma$C$^\delta$ coupling constant (ca. 70 Hz) is substantially larger than all of the phenylalanine aromatic $^1J_{CC}$ couplings (ca. 55 Hz) (Tran-Dinh et al., 1975). As expected, in ^{1}H-^{13}C spectra of both III^{Glc} (Fig. 1A) and P-III^{Glc} (Fig. 1B) acquired without decoupling during the acquisition period, a pair of doublets with large $^1J_{CH}$ couplings appear downfield of the phenylalanine signals and are therefore assigned as the two histidine ^{13}C$^{\epsilon 1}$-H resonances. Another pair of signals in the ^{1}H-^{13}C HMQC spectrum of III^{Glc} at ^{13}C chemical shifts of 119.1 ppm and 128.0 ppm (Fig. 1A) (118.7 ppm and 123.1 ppm in P-III^{Glc}; Fig. 1B) each exhibit a large $^1J_{CH}$ coupling in addition to a single $^1J_{CC}$ coupling, and are therefore assigned as the two histidine ^{13}C$^{\delta 2}$-H signals. Note that, in contrast with the other ^{13}C$^{\delta 2}$-H signals observed in Figure 1A and B, the ^{13}C$^{\delta 2}$-H signal of His-90 in III^{Glc} is not a well-resolved doublet. This is due the small chemical shift difference between His-90 ^{13}C$^\gamma$ and ^{13}C$^{\delta 2}$ (ca. 0.1 ppm), resulting in strong coupling between these spins.

Sequential signal assignments for His-75 and His-90

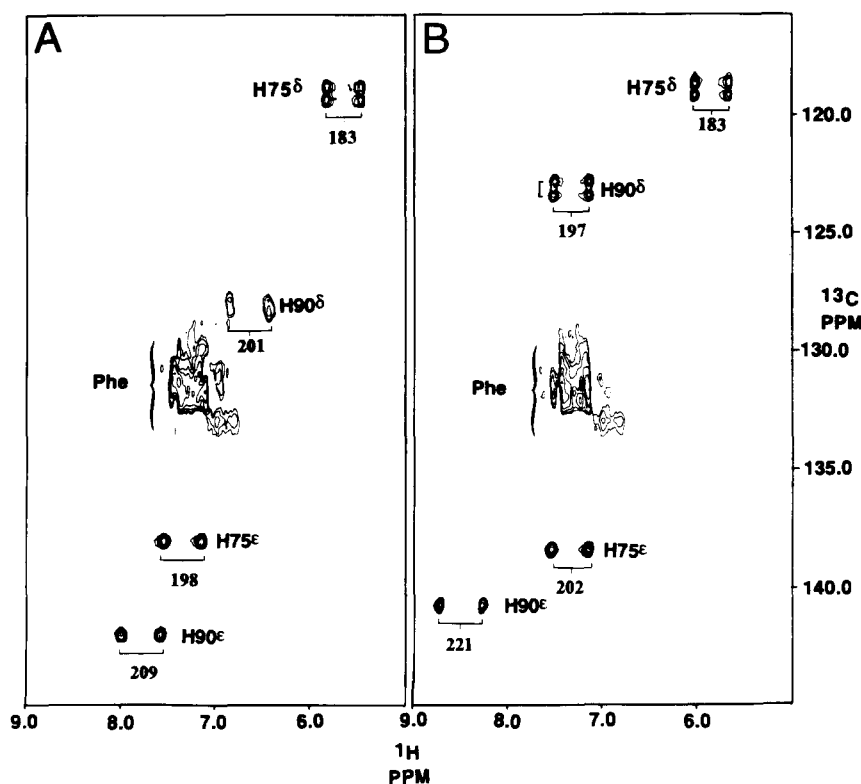Sequential assignments for the ^{13}C$^{\delta 2}$-H signals of His-75 and His-90 were obtained from a 2D ^{13}C CCH-COSY

Fig. 1. Downfield portions of ^{1}H-^{13}C HMQC spectra of III^{Glc}NC (308 K, pH 6.22) (**A**) and P-III^{Glc}NC (308 K, pH 6.24) (**B**) acquired without ^{13}C decoupling during the acquisition period. The delay during which ^{1}H and ^{13}C signals becomes antiphase was tuned to slightly less than $1/^1J_{CC}$ ($^1J_{CC} \sim 155$ Hz) to attenuate phenylalanine aromatic signals relative to histidine imidazole signals ($^1J_{CC}$ range 180–220 Hz). Peak assignments are denoted by a one-letter amino acid code, residue number, and Greek symbol. Imidazole $^1J_{CH}$ coupling constants (in Hz) are indicated under each signal.

experiment. Previously, we had assigned nearly all of the ^{1}H and ^{13}C side-chain signals of both III^{Glc} and P-III^{Glc}, including the H$^\beta$ signals of His-75 and His-90, using 3D HCCH-COSY (Bax et al., 1990a; Kay et al., 1990) and HCCH-TOCSY (Bax et al., 1990b; Clore et al., 1990) spectra (Pelton et al., 1991b). In contrast with the 3D experiment, in the 2D ^{13}C CCH-COSY experiment magnetization originates from the ^{13}C spins and is transferred from each histidine ^{13}C$^\gamma$ carbon to its directly bonded ^{13}C$^\beta$ and ^{13}C$^{\delta 2}$ carbons. In a subsequent step, the ^{13}C$^\gamma$-derived magnetization is transferred to the histidine H$^\beta$ and H$^{\delta 2}$ spins. Thus, the experiment correlates the ^{13}C$^\gamma$ signal of each histidine residue with its H$^{\delta 2}$ and H$^\beta$ signals. Because the H$^\beta$ sequential assignments are known, the observed correlations can be used to extend the sequential assignments to the H$^{\delta 2}$ signals. For example, in Figure 2A, at the ^{13}C chemical shift of 137.4 ppm, cross peaks are observed to the H$^\beta$ signals of His-75 (1.25 ppm and 2.70 ppm), and one of the two H$^{\delta 2}$ signals (5.63 ppm) identified in the ^{1}H-^{13}C HMQC spectrum (Fig. 1A). From these data the ^{13}C$^\gamma$ signal of His-75 can be assigned to 137.4 ppm, and the H$^{\delta 2}$ proton of His-75 can be assigned to 5.63 ppm. Similar correlations between the ^{13}C$^\gamma$ signal at 128.1 ppm with both the H$^\beta$ signals (1.94 ppm, 2.46 ppm) of His-90 and the second H$^{\delta 2}$ signal (6.64 ppm) identified in the ^{1}H-^{13}C HMQC spectrum (Fig. 1A) implies that His-90 ^{13}C$^\gamma$ resonates at 128.1 ppm and that His-90 H$^{\delta 2}$ resonates at 6.64 ppm. The ^{13}C chemical shifts are summarized in Table 1.

The 2D ^{13}C CCH-COSY spectrum provides similar information for the phenylalanine residues. For example, correlations appear (Fig. 2) between several of the phenylalanine ^{13}C$^\gamma$ signals (near 140 ppm) and their corresponding H$^\delta$ and H$^\beta$ signals (Fig. 2), confirming previous assignments based on homonuclear TOCSY spectra of unlabeled III^{Glc} (Pelton et al., 1991b). Correlations are also observed between several of the phenylalanine ^{13}C-ring signals and both their attached protons and their ^{1}H neighbors. However, the limited chemical shift dispersion of the phenylalanine ring ^{13}C and ^{1}H signals limits the utility of this experiment in sequential assignment of these spin systems.

Tautomeric states of His-75 and His-90

It remains to sequentially assign the ^{15}N$^{\delta 1}$, ^{15}N$^{\epsilon 2}$, and ^{13}C$^{\epsilon 1}$-H signals of His-75 and His-90. ^{15}N NMR spectroscopy has been used extensively to study the imidazole ring of histidine (Blomberg et al., 1977; Bachovchin & Roberts, 1978; Harbison et al., 1981; Munowitz et al., 1982; Roberts et al., 1982; Bachovchin, 1986). To simplify the discussion, the terms type-α, type-α+, and type-β have been introduced to describe the protonation state of a particular nitrogen (Table 2) (Witanowski et al., 1972; Bachovchin, 1986). In studies of histidine and model compounds it has been shown that type-α, type-α+, and type-β nitrogens have characteristic chemical shifts (Witanowski et al., 1972; Blomberg et al., 1977; Harbison
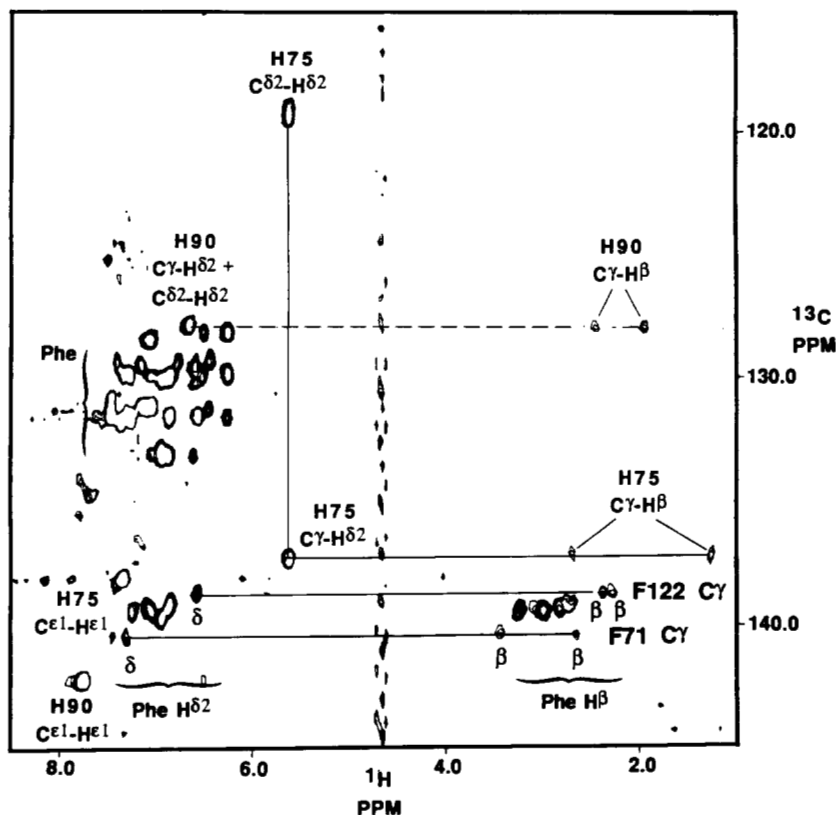
Fig. 2. Downfield portion of a ^{13}CCH-COSY spectrum of III^{Glc}NC (308 K, pH 7.50) showing histidine and phenylalanine ring signals. Correlations for His-75 and His-90 are denoted by solid and dashed lines, respectively. Phe ^{13}C$^\gamma$-H$^\delta$ and ^{13}C$^\gamma$-H$^\beta$ correlations are shown for F71 and F122.

et al., 1981; Munowitz et al., 1982; Roberts et al., 1982) (Table 2). Using these data the tautomeric states of the histidines in a number of proteins including α-lytic protease (Bachovchin & Roberts, 1978), triosephosphate isomerase (Lodi & Knowles, 1991), HPr (van Dijk et al., 1990), *E. coli* Enzyme-IIA^{mtl} (van Dijk et al., 1992), and *E. coli* β-hydroxydecanoyl thiolester dehydrase (Annand et al., 1992) have been determined. Moreover, in a detailed ^{15}N NMR study of histidine it was shown that the imid-

azole ring two-bond $^2J_N\delta1_H\epsilon1$, $^2J_N\epsilon2_H\epsilon1$, and $^2J_N\epsilon2_H\delta2$ coupling constants are ca. -10, -8, and -5.6 Hz, respectively, under basic conditions, whereas the three-bond $^3J_N\delta1_H\delta2$ coupling is -2 Hz (Blomberg et al., 1977). Because the $N^{\epsilon2}$-H tautomer is the most stable species of histidine under these conditions (Reynolds et al., 1973; Blomberg et al., 1977), the measured coupling constants primarily reflect those of the imidazole ring in the $N^{\epsilon2}$-H state (Blomberg et al., 1977). In spite of the size of III^{Glc}

Table 1. *Expected and observed ^{13}C chemical shifts for III^{Glc} and P-III^{Glc}*

| | Expected chemical shift[a] (ppm): tautomer | | | Observed chemical shift[b] (ppm) | | | |
| | | | | III^{Glc} | | P-III^{Glc} | |
Ring carbon	$N^{\epsilon2}$-H	$N^{\delta1}$-H	$N^{\epsilon2}$-H/$N^{\delta1}$-H	His-75	His-90	His-75	His-90
C$^\gamma$	136.8	128.8	129.7	137.4	128.1	137.4[c]	ND[d]
C$^{\delta2}$	121.9	128.5	120.2	119.1	128.0	118.7	123.1
C$^{\epsilon1}$	140.9	141.3	136.5	138.0	142.1	138.5	140.9
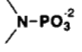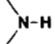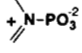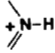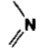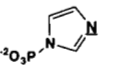
[a] Expected ^{13}C chemical shifts for the $N^{\delta1}$-H tautomer, the $N^{\epsilon1}$-H tautomer, and the cationic species were derived from solution NMR studies of $N^{\delta1}$-methylhistidine, $N^{\epsilon2}$-methylhistidine, and cationic L-histidine (Reynolds et al., 1973) and were recalculated from a benzene standard to a 3-[2,2,3,3-^{2}H$_4$]-trimethylsilylpropionate (TSP) standard by adding 128.7 ppm (to trimethylsilane [TMS]) (Stothers, 1972), and 1.9 ppm (to TSP).

[b] Chemical shifts for the ^{13}C$^\gamma$ signals of His-75 and His-90 (III^{Glc}) were measured at pH 7.50 in a 2D ^{13}C CCH-COSY spectrum, while ^{13}C$^{\delta2}$ and ^{13}C$^{\epsilon1}$ signals were obtained from ^{13}C HMQC spectra at pH 6.85 (III^{Glc}) and pH 6.74 (P-III^{Glc}).

[c] Determined from a 2D ^{13}C CCH-COSY spectrum of P-III^{Glc} (pH 7.77).

[d] ND, not determined.

Table 2. *Nitrogen types and characteristic*
^{15}N chemical shifts (ppm)^a

Structure	Nitrogen type	Chemical shift^b	Structure	Chemical shift^c
			$\backslash$N-PO$_3^{-2}$	202.1
$\backslash$N-H	α	167.5		
			$+\backslash$N-PO$_3^{-2}$	209.6
$+\backslash$N-H	α+	176.5		
			$^{-2}$O$_3$P-N$^+$-N-H (imidazole)	174.4
$\backslash$N	β	249.5		
			$^{-2}$O$_3$P-N-N (imidazole)	244.4

^{a} ^{15}N chemical shifts are referenced to liquid NH$_3$ and were recalculated from 1 M HNO$_3$ by subtracting reported values from 377.5 ppm (Witanowski et al., 1986).
^{b} Expected ^{15}N chemical shifts were derived from solution NMR studies of model compounds (Witanowski et al., 1972; Blomberg et al., 1977; Bachovchin & Roberts, 1978; Roberts et al., 1982; Bachovchin, 1986) and are consistent with solid-state NMR studies of imidazole and histidine (Harbison et al., 1981; Munowitz et al., 1982).
^{c} Expected ^{15}N shifts for *N*-phosphohistidine are based on solution NMR studies of *N*-phosphoimidazole and *N*-phospho-*N*-methylimidazole (van Dijk et al., 1990).

(18.1 kDa), it is expected that the imidazole ^{15}N and ^{1}H T$_2$s are large enough that these couplings will produce observable correlations in ^{1}H-^{15}N HMQC spectra, thus allowing for assignment of the ^{15}N$^{\delta1}$, ^{15}N$^{\epsilon2}$, and ^{13}C$^{\epsilon1}$-H signals.

By combining the ^{15}N chemical shift and J-coupling information, it is possible to construct the cross-peak patterns expected in ^{1}H-^{15}N HMQC spectra for histidine in the three different protonation states (Fig. 3). In modeling the spectra, it is important to note that the intensity of a cross peak depends on the coupling constant J in the following way, neglecting relaxation effects:

$$\text{peak intensity} \propto \sin^2(\pi J \tau), \qquad (1)$$

where τ is the mixing period during which ^{1}H and ^{15}N signals become antiphase (in our case 22 ms). Thus, for the N$^{\epsilon2}$-H tautomer (Fig. 3B), we expect a single strong N$^{\delta1}$-H$^{\epsilon1}$ correlation at a nitrogen chemical shift near

250 ppm, and we expect slightly weaker N$^{\epsilon2}$-H$^{\epsilon1}$ and N$^{\epsilon2}$-H$^{\delta2}$ correlations at a nitrogen chemical shift near 168 ppm. In contrast, for the N$^{\delta1}$-H tautomer (Fig. 3A) the opposite pattern is expected. First, the N$^{\delta1}$ and N$^{\epsilon2}$ nitrogen chemical shifts are expected to be inverted (Table 2). In addition, although coupling constants for the N$^{\delta1}$-H tautomer have not been measured, in general, it is expected that a type-β nitrogen will couple more strongly to the carbon-bound imidazole protons than a type-α or type-α+ nitrogen because of contributions due to the lone-pair electrons (Blomberg et al., 1977). Hence, for the N$^{\delta1}$-H tautomer the correlations between the type-β N$^{\epsilon2}$ and both H$^{\epsilon1}$ and H$^{\delta2}$ should be stronger than the correlation between the type-α N$^{\delta1}$ and H$^{\epsilon1}$ (Fig. 3A). In addition, based upon measured coupling constants in ring-protonated histidine (as a model), one expects that the three-bond ^{3}J$_N\delta1_H\delta2$ coupling for the N$^{\delta1}$-H tautomer to increase to ca. −3 Hz (Blomberg et al., 1977). If this is the case, then a weak N$^{\delta1}$-H$^{\delta2}$ correlation will be observed (Fig. 3A). Finally, the chemical shifts and cou-
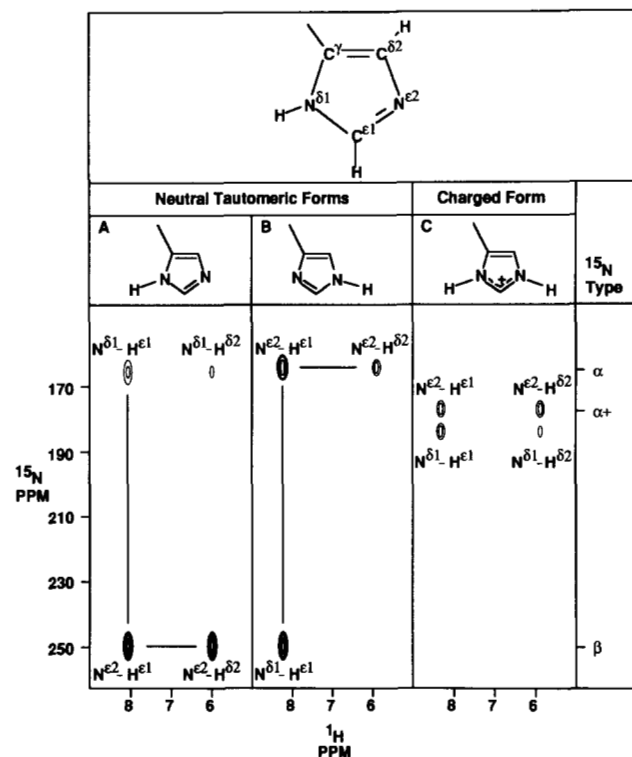
Fig. 3. Schematic diagram showing the nomenclature used to describe the imidazole atoms, the three possible protonation states of the histidine ring, and the expected ^{1}H-^{15}N HMQC spectrum of each species. The spectra were constructed using ^{15}N chemical shifts taken from Table 2, and both ^{2}J$_{NH}$ and ^{3}J$_{NH}$ coupling constants of histidine (Blomberg et al., 1977). Note that for the charged species, the spectrum was constructed with the N$^{\delta1}$ signal slightly downfield of the N$^{\epsilon2}$ signal. In practice either nitrogen could resonate downfield of the other, and the assignments must be made through a comparison of cross-peak intensities.

pling constants observed for histidine at low pH (Blomberg et al., 1977) indicate that the signal pattern shown in Figure 3C will be observed for protonated, cationic histidine. Because the chemical shifts of $N^{\delta 1}$ and $N^{\epsilon 2}$ are nearly the same, the NMR signal pattern easily distinguishes this form of histidine from either of the two neutral tautomeric forms. It should be noted that the above arguments regarding the signal intensities were made neglecting relaxation effects. In general the most intense signals will be observed for histidine residues having the largest ^{15}N and ^1H T_2 values, such as a residue having a highly flexible side chain.

Recently van Dijk et al. (1992) have used ^1H-^{15}N HMQC experiments to identify the tautomeric forms of the histidines in Enzyme-IIA^{mtl}. Our analysis of the HMQC data differs from theirs in one significant respect. As detailed above, we assert that the weak cross peaks observed in ^1H-^{15}N HMQC spectra at the chemical shifts of $N^{\delta 1}$ and $H^{\delta 2}$ result from the relatively small three-bond $^3J_{N^{\delta 1}H^{\delta 2}}$ coupling (Blomberg et al., 1977) rather than from exchange processes as suggested (van Dijk et al., 1992). In particular, in the previous study a cross peak at the chemical shifts of $N^{\delta 1}$ and $H^{\delta 2}$ is observed for His-B of Enzyme-IIA^{mtl} (van Dijk et al., 1992). This peak cannot be explained using fast-exchange-based arguments. That this signal results from a weak $^3J_{N^{\delta 1}H^{\delta 2}}$ coupling is not surprising when it is noted that the signals for His-B are characterized by long T_2s (intense cross peaks) and

that in such a case observation of cross peaks due to weaker couplings is more favorable. Finally, as stated above, we expect the $J_{N^{\delta 1}H^{\delta 2}}$ coupling to increase when the ring exists in the $N^{\delta 1}$-H tautomeric state, making the appearance of a $N^{\delta 1}$-$H^{\delta 2}$ cross peak more likely (see below).

^1H-^{15}N HMQC spectra of III^{Glc} and P-III^{Glc} acquired at pH ca. 8.3 are shown in Figure 4. For unphosphorylated III^{Glc} (Fig. 4A) it can be seen that the previously assigned $H^{\delta 2}$ signal of His-90 (6.64 ppm; Fig. 1) is strongly correlated with a type-β nitrogen at 243.5 ppm, and that this nitrogen is strongly correlated with one of the two $H^{\epsilon 1}$ signals identified in the ^1H-^{13}C HMQC spectrum (7.78 ppm; Fig. 1). In addition, correlations can be seen between a type-α nitrogen at 168.8 ppm and both the $H^{\delta 1}$ signal of His-90 and the aforementioned $H^{\epsilon 1}$ signal. Comparison of this cross-peak pattern with the expected results (Fig. 3A) shows that His-90 exists predominantly as the $N^{\delta 1}$-H tautomer. In contrast it can be seen in Figure 4A that His-75 $H^{\delta 2}$ (5.63 ppm, Fig. 1) is correlated to a type-α nitrogen at 164.5 ppm. Furthermore, the second $H^{\epsilon 1}$ signal (7.33 ppm) identified in Figure 1 is strongly correlated with a type-α nitrogen at 164.5 ppm as well as with a type-β nitrogen at 245.0 ppm. Comparison of this cross-peak pattern with the expected results (Fig. 3B) shows that His-75 exists predominantly in the $N^{\epsilon 2}$-H state. The ^1H and ^{15}N chemical shifts are summarized in Tables 3 and 4.

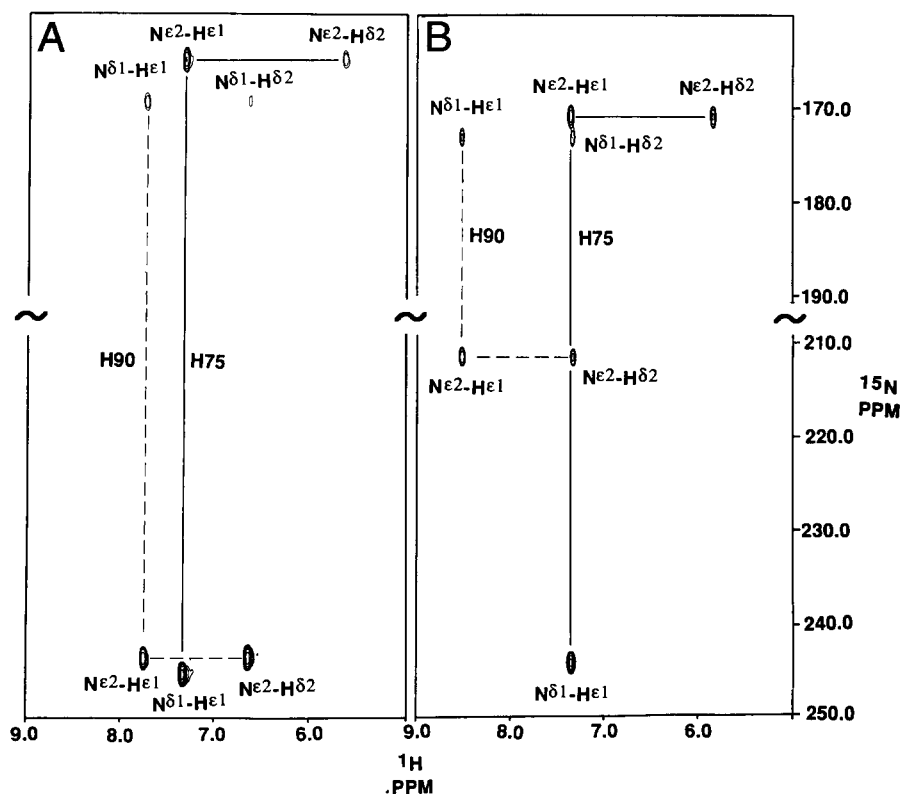Fig. 4. Portions of ^1H-^{15}N HMQC spectra of III^{Glc}N (pH 8.30) (A) and P-III^{Glc}N (pH 8.43) (B) acquired in D$_2$O. The cross-peak patterns for His-75 (solid line) and His-90 (dashed line) are shown. The delay during which ^1H and ^{15}N signals become antiphase was set to 22 ms ($2/^1J_{NH}$) to refocus single-bond correlations. Nitrogen and proton assignments are denoted by Greek symbols.

Table 3. *Histidine imidazole ^1H chemical shifts in III^{Glc} and P-III^{Glc} (ppm)*[a]

		$H^{\delta 1}$	$H^{\delta 2}$	$H^{\varepsilon 1}$	$H^{\varepsilon 2}$
III^{Glc b}	His-75	NA	5.63	7.33	ND
	His-90	10.74	6.64	7.78	NA
P-III^{Glc c}	His-75	NA	5.79	7.31	13.65
	His-90	11.58	7.29	8.48	NA

[a] Abbreviations: NA, not applicable; ND, not determined.

[b] Chemical shifts measured at pH 6.22, except for His-90 $H^{\delta 1}$, which was measured at pH 8.78.

[c] Chemical shifts measured at pH 6.24, except His-90 $H^{\delta 1}$ and His-75 $H^{\varepsilon 2}$, which were measured at pH 8.60.

^{15}N NMR studies of N-phosphoimidazole and N-methyl-N-phosphoimidazole indicate that a phosphorylated nitrogen should resonate between 202 ppm and 209 ppm, depending on whether the ring is cationic or neutral (van Dijk et al., 1990). As noted previously, His-90 is phosphorylated at the $N^{\varepsilon 2}$ position (Meadow & Roseman, 1982; Dörschug et al., 1984), and therefore His-90 $N^{\varepsilon 2}$ is expected to show the chemical shift of a phosphorylated ^{15}N spin. In the ^1H-^{15}N HMQC spectrum of P-III^{Glc} (Fig. 4B), a single nitrogen resonates at 211.5 ppm and can be assigned to $N^{\varepsilon 2}$ of P-His-90. It follows that the downfield pair of $H^{\delta 2}$ and $H^{\varepsilon 1}$ signals ($H^{\delta 2}$, 7.29 ppm; $H^{\varepsilon 1}$, 8.48 ppm) belong to His-90, and that the cross-peak pattern associated with the upfield set of proton signals ($H^{\delta 2}$, 5.79 ppm, $H^{\varepsilon 1}$, 7.31 ppm) corresponds to His-75. The ^1H and ^{15}N chemical shifts derived from this spectrum of P-III^{Glc} are summarized in Tables 3 and 4.

It is evident from comparison of predicted and observed ^{15}N chemical shifts for P-III^{Glc} (Table 4) that $N^{\varepsilon 2}$ and $N^{\delta 1}$ of His-90 resonate close to the chemical shifts expected for the phosphorylated and nonphosphorylated

nitrogens, respectively, of a phosphoimidazolium moiety. In contrast, for His-75, the $N^{\delta 1}$ and $N^{\varepsilon 2}$ chemical shifts are nearly identical in the phosphorylated and unphosphorylated proteins (Fig. 4; Table 4), and it can be concluded that His-75 remains in the $N^{\varepsilon 2}$-H tautomeric state.

To confirm and extend the experiments just described, attempts were made to directly observe the imidazole ^{15}N-H signals in ^1H-^{15}N spectra. In general, imidazole NH protons exchange rapidly with solvent and are not observable (Wüthrich, 1986). However, in cases where the exchange rate is slowed, for instance because of hydrogen bonding or inaccessibility to solvent, these signals may be observed in spectra acquired without solvent presaturation. ^1H-^{15}N HMQC spectra acquired with a 1:1 echo solvent suppression scheme (Bax et al., 1990c) are shown in Figure 5. For the unphosphorylated protein (Fig. 5A), comparison of the observed signal with the ^{15}N assignments (Table 4) shows that the proton at 10.74 ppm is attached to $N^{\delta 1}$ of His-90. In making the comparison, we note that the ^{15}N signals in Figure 5 are downfield shifted ca. 0.5 ppm from those of Figure 4 due to a ^2H isotope effect (Hansen, 1983). Observation of the $N^{\delta 1}$-$H^{\delta 1}$ signal confirms the conclusion based on ^{15}N chemical shifts that the $N^{\delta 1}$ nitrogen of His-90 is protonated (Table 4). In contrast, the expected $N^{\varepsilon 2}$-$H^{\varepsilon 2}$ signal of His-75 was not observed. This suggests that His-75 $H^{\varepsilon 2}$ exchanges more rapidly with solvent than does His-90 $H^{\delta 1}$.

Before collecting similar spectra of the phosphorylated protein, a spectrum of III^{Glc} dissolved in 0.15 M KCl and containing all of the components needed for phosphorylation except for Enzyme I was recorded and observed to be identical to that of III^{Glc} recorded in 0.15 M KCl alone. After phosphorylation of the protein, through the addition of Enzyme I (5 units), two signals were observed (Fig. 5B). Comparison of the data with the previous ^{15}N assignments (Table 4) shows that the proton at 13.65 ppm

Table 4. *Expected and observed imidazole ^{15}N chemical shifts for III^{Glc} and P-III^{Glc}*[a]

Residue		Nitrogen	Protonation state	Observed shift (ppm)	Expected shift[b] (ppm)	Difference (ppm)
III^{Glc}	His-75	$N^{\delta 1}$	Unprotonated	245.0	249.5	−4.5
		$N^{\varepsilon 2}$	Protonated	164.5	167.5	−3.0
	His-90	$N^{\delta 1}$	Protonated	168.8	167.5	1.3
		$N^{\varepsilon 2}$	Unprotonated	243.5	249.5	−6.0
P-III^{Glc}	His-75	$N^{\delta 1}$	Unprotonated	243.9	249.5	−5.6
		$N^{\varepsilon 2}$	Protonated	170.8	167.5	3.3
	His-90	$N^{\delta 1}$	Protonated	172.9	174.4	−1.5
		$N^{\varepsilon 2}$	Phosphorylated	211.5	209.6	1.9

[a] ^{15}N chemical shifts are referenced with respect to liquid NH_3.

[b] Expected ^{15}N chemical shifts were derived from solution NMR studies of model compounds (Witanowski et al., 1972; Blomberg et al., 1977; Bachovchin & Roberts, 1978; Roberts et al., 1982; van Dijk et al., 1990). Expected chemical shifts were recalculated from 1 M HNO_3 by subtracting reported values from 377.5 ppm (Witanowski et al., 1986).
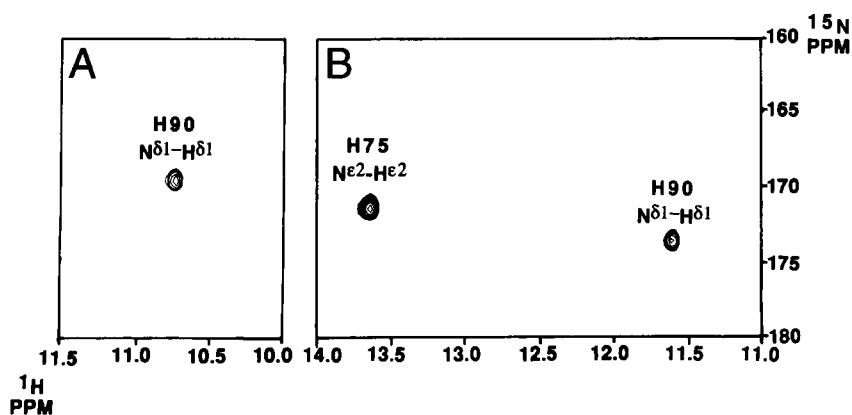
Fig. 5. Portions of ^1H-^{15}N HMQC spectra of III^{Glc}N (308 K, pH 8.78) and P-III^{Glc}N (308 K, pH 8.60) acquired in H_2O with a 1-1 echo suppression sequence (Bax et al., 1990c). The imidazole ^{15}N-^1H signals are denoted by residue number. Note that the ^{15}N signals in this spectrum are downfield shifted ca. 0.5 ppm compared to the ^1H-^{15}N HMQC spectra acquired in D_2O (Fig. 4) because of an ^2H isotope effect (Hansen, 1983).

is attached to $N^{\varepsilon 2}$ of His-75, and that the proton at 11.58 ppm is attached to $N^{\delta 1}$ of His-90, confirming that these nitrogens are protonated as predicted (Table 4). Interestingly, as can be seen by comparison of Figure 5A and B, that the $N^{\varepsilon 2}$-H signal of His-75 is observed in spectra of P-III^{Glc} but not in spectra of III^{Glc}. This is probably due to a reduced rate of exchange of His-75 $N^{\varepsilon 2}$-H with solvent in the phosphorylated protein, possibly due to hydrogen bond formation (see below).

Imidazole ring ^{13}C chemical shifts, particularly those of $^{13}C^\gamma$, acquired as a function of pH have also been used to determine the tautomeric states of histidine residues (Roberts et al., 1973; Walters & Allerhand, 1980). In Table 1, the data of Reynolds et al. (1973) are summarized along with the observed ^{13}C chemical shifts for His-75 and His-90 in III^{Glc} and P-III^{Glc}. Comparison of expected and observed ^{13}C chemical shifts for the unphosphorylated protein confirms that His-75 exists predominantly as the $N^{\varepsilon 2}$-H tautomer and that His-90 exists predominantly as the $N^{\delta 1}$-H tautomer, in agreement with the results based on ^{15}N chemical shifts (Table 4). In particular, the large difference in $^{13}C^\gamma$ and $^{13}C^{\delta 2}$ chemical shifts expected for the $N^{\varepsilon 2}$-H tautomer (14.9 ppm) is observed for His-75 (18.3 ppm), and the small chemical shift difference expected in these signals for the $N^{\delta 1}$-H tautomeric state (0.3 ppm) is observed for His-90 (0.1 ppm). Similarly, ^{13}C chemical shifts for His-75 in P-III^{Glc} are consistent with its being predominantly in the $N^{\varepsilon 2}$-H state, in agreement with our previous conclusions. At present, information on ^{13}C chemical shifts for phosphohistidine model compounds is unavailable, and it is therefore not possible to determine the protonation state of His-90 using ^{13}C NMR spectroscopy. We note in passing, however, that the $^{13}C^{\delta 2}$ signal of His-90 shifts upfield by 4.9 ppm upon phosphorylation (Fig. 1; Table 1).

Charge states of the active-site histidines

Imidazole ^1H, ^{13}C, and ^{15}N chemical shifts for His-75 and His-90 derived from ^1H-^{15}N HMQC and ^1H-^{13}C

HMQC spectra of III^{Glc} and P-III^{Glc} were measured at several pH values to determine the pK_a for each ring (Supplementary material, Diskette Appendix). Before studying the phosphorylated protein, ^1H-^{15}N HMQC spectra of III^{Glc} dissolved in 0.15 M KCl and all of the components needed for phosphorylation except Enzyme I were recorded at various pH values ranging from 6.0 to 9.0. These spectra were identical to those obtained with III^{Glc} dissolved in 0.15 M KCl, indicating that the cocktail used for phosphorylation did not significantly affect the titration behavior of either histidine residue over the pH range studied.

The histidine imidazole ^1H signals of both His-75 and His-90 in III^{Glc} and P-III^{Glc} are invariant with respect to pH changes of the bulk solution over the range from 6.0 to 9.0. In addition, the imidazole ^{15}N signals of His-75 in III^{Glc} and both His-75 and His-90 in P-III^{Glc} are insensitive to pH changes (pH range 6.0–9.0). Similarly, no changes in the imidazole ^{13}C signals were observed for either histidine residue in either form of the protein. Surprisingly, only the $^{15}N^{\delta 1}$ and $^{15}N^{\varepsilon 2}$ signals of His-90 in the unphosphorylated protein exhibited shifts at low pH values (pH 6.3), and these shifts were minor. In particular, His-90 $N^{\delta 1}$ shifted downfield 0.9 ppm when the pH was lowered from 9.11 to 6.24. Conversely, His-90 $N^{\varepsilon 2}$ shifted upfield 3.4 ppm when the pH is lowered over the same range. These small shifts suggest the onset of protonation of the imidazole ring of His-90 and imply that the pK_a value of His-90 is greater than that of His-75. The pH study was not extended to either higher or lower pH values because of protein aggregation below pH 6.0 and inefficient regeneration of the phosphorylated protein above pH 9.0.

The pH dependence of the histidine imidazole signals in III^{Glc} and P-III^{Glc} contrast with data obtained for histidine incorporated into short peptides. Typically, in peptides, the $^1H^{\varepsilon 1}$ and $^1H^{\delta 2}$ signals shift upfield by 0.8 ppm and 0.4 ppm, respectively, upon protonation with a pK_a of 7.0 (Bundi & Wüthrich, 1979). Imidazole $^{15}N^{\delta 1}$ and $^{15}N^{\varepsilon 2}$ signals have also been shown to undergo large

chemical shift changes (type-β to type-$\alpha+$, 73 ppm upfield shift; type-α to type-$\alpha+$, 9 ppm downfield shift) upon protonation (Witanowski et al., 1972; Blomberg et al., 1977; Bachovchin & Roberts, 1978) (Table 2), whereas $^{13}C^{\epsilon 1}$ signals undergo smaller changes (3 ppm) (Richarz & Wüthrich, 1978). Thus, the invariance of the imidazole signals of His-75 and His-90 in both the phosphorylated and unphosphorylated forms of III^Glc to changes in pH indicate that the protonation states of these histidines remain unchanged in the pH range from 6.0–9.0.

Phosphoryl group–amide proton interactions

It has been postulated that the amide protons of Asp-94, Thr-95, and Val-96 interact with the phosphoryl oxygen atoms (Liao et al., 1991; Worthylake et al., 1991). To further elucidate this issue, approximate exchange rates for Asp-94, Thr-95, and Val-96 in both III^Glc and P-III^Glc were obtained. When III^Glc is dissolved in both 0.15 M KCl and in 0.15 M KCl with all other buffer components needed for phosphorylation except Enzyme I, no signals for Asp-94, Thr-95, or Val-96 are observed in ^{15}N HSQC spectra acquired 6.25 min after addition of D_2O (Supplementary material) (pH 6.64). This indicates that the half-life for exchange of these protons is less than ca. 2.5 min. However, in similar experiments conducted at the same pH (6.64) but with the phosphorylated protein, the amide signals of Asp-94 and Thr-95 are observable in spectra acquired 7.5 min after addition of D_2O and disappear after 13.5 min, whereas the amide signal of Val-96 is not observed in even the first spectrum (7.5 min) (Supplementary material). These data indicate that the half-lives of Asp-94 and Thr-95 (>4 min) increase as a result of phosphorylation.

Discussion

A number of techniques have been used to assign the ^1H, ^{15}N, and ^{13}C signals of the imidazole ring of histidine (Markley, 1975; Wang et al., 1990). A particularly popular method is to assign the ^{15}N signals through comparison of 1D ^{15}N spectra of mutant proteins that contain a single histidine residue labeled only at $N^{\delta 1}$ or at both $N^{\delta 1}$ and $N^{\epsilon 2}$ (Bachovchin, 1986; van Dijk et al., 1990; Lodi & Knowles, 1991; Annand et al., 1992). Because of the low sensitivity of the ^{15}N nucleus, collection of ^{15}N spectra is time-consuming, especially if data are needed at multiple pH values. More recently 2D ^1H-^{15}N HMQC experiments have been applied to an Enzyme-II^mtl preparation (van Dijk et al., 1992) in which the histidine ring nitrogens were specifically labeled with ^{15}N. In our approach a single set of uniformly ^{15}N- and ^{15}N/^{13}C-labeled samples is used in combination with 2D ^1H-^{13}C HMQC, ^1H-^{13}C CCH-COSY and ^1H-^{15}N HMQC spectra to sequentially assign the histidine ring ^1H, ^{15}N, and ^{13}C signals. In addition, the pH titration behavior of the ^1H,

^{15}N, and ^{13}C signals is recorded efficiently because high sensitivity spectra are typically recorded in 2 h. Finally, we note that our approach does not require the preparation of labeled samples beyond those needed to obtain complete signal assignments.

Recent X-ray (Worthylake et al., 1991) and NMR (Pelton et al., 1991a,b, 1992) structural studies of III^Glc from *E. coli* and the homologous IIA domain from *B. subtilis* (Fairbrother et al., 1991a,b, 1992; Liao et al., 1991) have provided insight into the structural features of the active sites of these proteins. The *B. subtilis* IIA domain has 42% sequence identity with *E. coli* III^Glc, and the two proteins have similar although not identical structures (Worthylake et al., 1991). Common to the active sites of both proteins is a pair of histidine residues surrounded by a number of hydrophobic groups. The two histidines, His-75 and His-90 in the *E. coli* protein, were found to be close in space, with the $N^{\epsilon 2}$ atoms only 3.3 Å apart. Moreover, the spatial orientations of the imidazole rings in both proteins were fixed owing to apparent hydrogen bonds between $N^{\delta 1}$ of His-75 (His-68 in *B. subtilis*) and the hydroxyl group of Thr-73 (Thr-66 in *B. subtilis*) and between $N^{\delta 1}$ of His-90 (His-83 in *B. subtilis*) and the carbonyl oxygen of Gly-92 (Gly-85 *B. subtilis*). Thus, for His-90, it was predicted that $N^{\delta 1}$ is a type-α nitrogen and acts as a hydrogen-bond donor to the carbonyl oxygen of Gly-92. However, for His-75, the nature of the hydrogen-bond was ambiguous (Liao et al., 1991; Worthylake et al., 1991). A type-α $N^{\delta 1}$ could act as a hydrogen-bond donor with the hydroxyl oxygen of Thr-73 as the acceptor. Conversely, a type-β His-75 $N^{\delta 1}$ could act as a hydrogen-bond acceptor with the hydroxyl group as the donor.

Active site of III^Glc

Our results on the tautomeric states of the histidine rings of III^Glc and P-III^Glc from *E. coli* are summarized in relation to the known structural features of the active site in Figure 6. It is clear from the ^{15}N chemical shift data for III^Glc (Fig. 4) that His-90 exists predominantly as the $N^{\delta 1}$-H tautomer (Fig. 6A), in contrast to L-histidine, which exists predominantly in the $N^{\epsilon 2}$-H state (Reynolds et al., 1973; Blomberg et al., 1977). It is also clear that His-75 exists predominantly as the $N^{\epsilon 2}$-H tautomer (Fig. 6). For His-90 the direct observation of the $N^{\delta 1}$-H signal in the ^1H-^{15}N HMQC spectrum of III^Glc (Fig. 5A) confirmed that this nitrogen was protonated. In contrast, the His-75 $N^{\epsilon 2}$-H signal was not observed (Fig. 5A). As stated previously, in general, imidazole NH protons exchange rapidly with solvent and, as a consequence, these signals are usually not observed unless the rate is slowed, for instance through hydrogen bonding or inaccessibility to solvent (Wüthrich, 1986). Formation of a hydrogen bond between His-90 $N^{\delta 1}$-H and Gly-92 CO as suggested (Liao et al., 1991; Worthylake et al., 1991) and lack of hydrogen bonding associated with His-75 $N^{\epsilon 2}$-H accounts
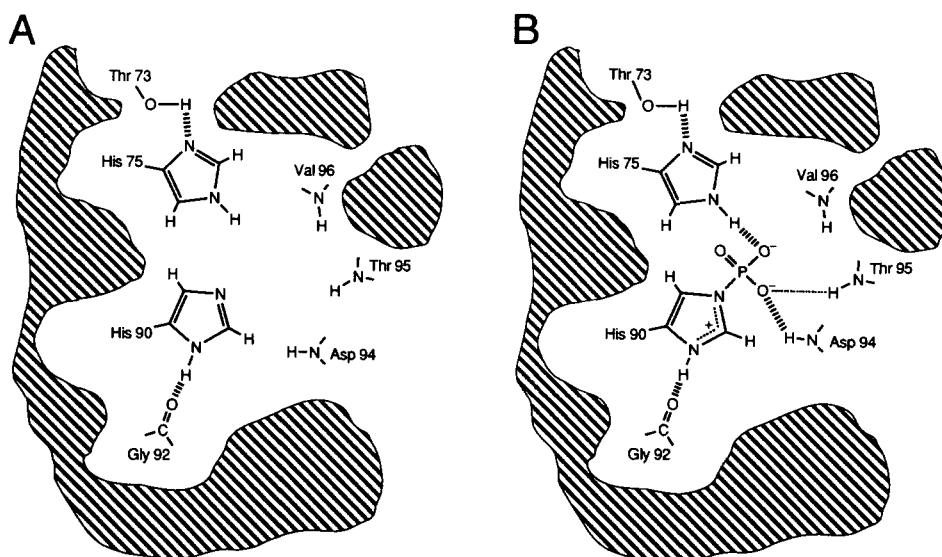
Fig. 6. Schematic diagram showing the tautomeric states of the active-site histidines of III^Glc (**A**) and P-III^Glc (**B**). The figure also depicts important structural features of the active site derived from studies of III^Glc from *E. coli* (Pelton et al., 1991a,b, 1992; Worthylake et al., 1991) and the IIA domain from *B. subtilis* (Fairbrother et al., 1991a,b, 1992; Liao et al., 1991). The shaded portion of the figure represents the ring of hydrophobic residues that surround the active-site histidines. The hydrogen bond between Thr-95 and the phosphoryl group (represented by a thin dashed line)(Fig. 6B) is less certain than that between Asp-94 and the phosphoryl group (see text).

for this difference in exchange rates (Fig. 6A). The His-90 $N^{\delta 1}$-H···Gly-92 CO hydrogen bond also accounts for the shift in the tautomeric equilibrium of His-90 to the less stable $N^{\delta 1}$-H form. Hydrogen-bonding schemes similar to that proposed for His-90 have been invoked to account for the fact that the active-site histidines of α-lytic protease (Bachovchin & Roberts, 1978) and *E. coli* β-hydroxydecanoyl thiolester dehydrase (Annand et al., 1992) adopt the less stable $N^{\delta 1}$-H tautomeric form. Finally, the fact that His-75 $N^{\delta 1}$ is unprotonated (type-β) (Table 4) in conjunction with the X-ray results indicates that this nitrogen ($N^{\delta 1}$) must act as a hydrogen-bond acceptor with the hydroxyl proton of Thr-73. Moreover, His-75 and His-90, as well as Thr-73 and Gly-92, are conserved in a number of PTS proteins and non-PTS permeases (Meadow et al., 1990; Liao et al., 1991). On this basis we would expect the histidines in these proteins to exist in the same tautomeric states and to form similar hydrogen-bonding networks.

The great advantage in using ^{15}N chemical shifts to determine the tautomeric states of histidine residues is due to the large chemical shift difference between a protonated (type-α or type-α+) and an unprotonated (type-β) nitrogen (Table 2). More recently, the presence of hydrogen bonds has been inferred from perturbations of ^{15}N chemical shifts from their canonical (non-hydrogen-bonded) values. In a detailed study of ^{15}N chemical shifts of nitrogens in imidazole-based model compounds (Schuster & Roberts, 1979; Roberts et al., 1982), it was shown that type-α and type-α+ nitrogens acting as hydrogen-bond donors show systematic downfield shifts (up to

10 ppm) relative to expected values (Table 2), whereas type-β nitrogens acting as hydrogen-bond acceptors show systematic upfield shifts (up to 10 ppm). These data have been used to show that His-57 $N^{\delta 1}$-H and His-57 $N^{\epsilon 2}$ of α-lytic protease are both involved in hydrogen bonds (Bachovchin, 1986).

As applied to III^Glc, the inference of hydrogen bonding based on small differences in ^{15}N chemical shifts from the canonical values is not completely consistent with the conclusions presented above. Inspection of Table 4 shows that His-75 $N^{\delta 1}$ is an unprotonated (type-β) nitrogen that resonates 4.5 ppm upfield of its canonical value. This observation is consistent with formation of a hydrogen bond between His-75 $N^{\delta 1}$ and the hydroxyl group of Thr-73 (Fig. 6A). In contrast, His-90 $N^{\delta 1}$ is type-α with a chemical shift close to its canonical value, whereas His-90 $N^{\epsilon 2}$ resonates 6 ppm upfield from the canonical type-β value (Table 4). Applying Bachovchin's hydrogen-bond analysis to this chemical shift data would imply that His-90 $N^{\delta 1}$-H is not a hydrogen-bond donor, and that His-90 $N^{\epsilon 2}$ is a hydrogen-bond acceptor, both of which are contrary to our conclusions based on the ^{1}H-^{15}N HMQC spectrum of III^Glc (Fig. 5A) combined with the X-ray structure of the protein (Liao et al., 1991; Worthylake et al., 1991). In this regard, it has been observed (Lodi & Knowles, 1991) that the type-β $N^{\delta 1}$ nitrogen of His-95 of triosephosphate isomerase exhibits a downfield shift of 6.7 ppm from its canonical value (Table 2), although any hydrogen bonding should cause an upfield shift. Similarly, the type-α $N^{\epsilon 2}$ nitrogen exhibits

an upfield shift of 3.5 ppm, although any hydrogen bonding should cause a downfield shift of this resonance.

Although the data on model compounds (Schuster & Roberts, 1979; Roberts et al., 1982) shows that hydrogen bonding influences ^{15}N chemical shifts, it is clear that in proteins, other, as yet undetermined, factors affect the ^{15}N shift to a comparable extent. Indeed, the amide ^{15}N resonances of Phe-77 and Phe-91 differ by 12.2 ppm in III^{Glc} (Pelton et al., 1991a), although both reside in β-sheet segments (Pelton et al., 1991a; Worthylake et al., 1991) and show slow rates of exchange indicative of hydrogen bonding (J.G.P. & D.A.T, unpubl. data). Thus, in light of the results obtained for III^{Glc} and triosephosphate isomerase (Lodi & Knowles, 1991), we believe that caution should be used in relating relatively small ^{15}N chemical shift changes to hydrogen bonding of imidazole rings in proteins.

Active site of P-III^{Glc}

The NMR results (Tables 1, 4; Fig. 6B) indicate that His-75 and His-90 remain protonated at $N^{\varepsilon 2}$ and $N^{\delta 1}$, respectively, upon phosphorylation. Recently we showed, using heteronuclear 3D NMR methods, that very little structural change occurs in III^{Glc} upon phosphorylation (Pelton et al., 1992). We therefore expect the hydrogen bonds between His-75 $N^{\delta 1}$ and Thr-73 hydroxyl group, and between His-90 $N^{\delta 1}$-H and Gly-92 carbonyl group to remain intact in the phosphorylated protein (Fig. 6B). Furthermore, it was predicted on the basis of model building and the X-ray structure of the IIA domain from *B. subtilis* (Liao et al., 1991) that $N^{\varepsilon 2}$-H of His-75 (*E. coli*) or His-68 (*B. subtilis*) would act as a hydrogen-bond donor to the phosphoryl oxygen atoms in the phosphorylated protein. In agreement with this prediction, one of the most striking experimental differences between III^{Glc} and P-III^{Glc} was our ability to detect the $N^{\varepsilon 2}$-H signal of His-75 in the phosphorylated state but not in the unphosphorylated state. This observation implies that the exchange rate for His-75 $H^{\varepsilon 2}$ is reduced in the phosphorylated protein as compared to the unphosphorylated protein. The reduced exchange rate is consistent with the His-75 $N^{\varepsilon 2}$-H group acting as a hydrogen-bond donor with the phosphoryl oxygen atoms, as predicted (Fig. 6B) (Liao et al., 1991). We also note that His-75 $N^{\varepsilon 2}$ shifts downfield 6.3 ppm upon phosphorylation (Table 4) consistent with hydrogen-bond formation.

For P-III^{Glc}, His-75 remains neutral upon phosphorylation. In contrast, the direct observation of the P-His-90 $^{15}N^{\delta 1}$-H signal (Fig. 5B) along with the ^{15}N chemical shift data (Table 4) show that His-90 $N^{\delta 1}$ is protonated. This, and the knowledge that His-90 $N^{\varepsilon 2}$ is phosphorylated (Meadow & Roseman, 1982; Dörschug et al., 1984), together imply that the imidazole ring of His-90 adopts a positive charge in the phosphorylated state. Hultquist et al. (1966) showed that the pK_a's for the phosphoryl

oxygens of L-$N^{\varepsilon 2}$-phosphohistidine are each less than 3.0, and therefore at pH 6.4 both oxygens are negatively charged. If the same holds for P-III^{Glc}, in which the phosphoryl group is on the surface of the protein exposed to solvent, then the overall charge on the P-His-90 moiety would be negative 1 (Fig. 6B).

Our model of the active site of P-III^{Glc} (Fig. 6B) includes Asp-94, Thr-95, and Val-96, whose amide protons have been postulated to interact with the phosphoryl oxygens (Liao et al., 1991; Worthylake et al., 1991). In our previous comparison of III^{Glc} and P-III^{Glc} we found that the amide protons of Asp-94 and Val-96 exhibited the largest downfield shifts upon phosphorylation, whereas the amide proton of Thr-95 exhibited only a minor shift (Asp-94, 0.68 ppm; Thr-95, 0.07 ppm; Val-96, 1.12 ppm) (Pelton et al., 1992). This is intriguing in light of the conclusions of Wagner et al. (1983) who have shown a correlation between downfield-shifted amide proton signals and strong hydrogen bonding (see also Redfield & Papastavros [1990]). It is also interesting to note that minor changes in the intensities of the NOEs associated with the amide protons of Asp-94 and Val-96, representing distance changes of less than 1.5 Å, were detected in our previous study of P-III^{Glc} (Pelton et al., 1992), whereas no changes were observed for Thr-95. For example, the NOE between the amide proton of Asp-94 and $H^{\varepsilon 1}$ of His-90 becomes slightly stronger upon phosphorylation, suggesting that this amide proton also shifts toward the phosphoryl oxygen atoms.

To further elucidate this issue, approximate exchange rates for these amide protons were determined for both III^{Glc} and P-III^{Glc}. For Asp-94, the reduced rate of exchange (half-life <2.5 min III^{Glc}; >4.0 min P-III^{Glc}), along with the large downfield shift of its amide proton, and the slight structural shift of this group observed in 3D ^1H-^{15}N NOESY-HMQC spectra (Pelton et al., 1992) are all consistent with formation of a hydrogen bond between this group and the phosphoryl oxygen atoms as predicted (Worthylake et al., 1991). However, for Thr-95 and Val-96 the data are less certain. The reduced rate of exchange of Thr-95 NH (half-life <2.5 min III^{Glc}; >4.0 min P-III^{Glc}) does suggest hydrogen-bond formation, although a large chemical shift change is not observed. Furthermore, the large downfield shift of Val-96 is consistent with hydrogen-bond formation; but the exchange rates for this proton in III^{Glc} and P-III^{Glc} are too fast to allow for differentiation in the two forms of the protein. Therefore, at present, we have included a hydrogen bond between Asp-94 NH and the phosphoryl oxygen atoms in our model of the active site and have also tentatively assigned a hydrogen bond between Thr-95 NH and the phosphoryl group (Fig. 6B). However, additional experiments will be needed to confirm whether Thr-95 and Val-96 really participate in such interactions.

It is evident from the invariance of the imidazole ^1H, ^{15}N, and ^{13}C chemical shifts with changes in pH that

the protonation states of His-75 and His-90 in III^{Glc} and P-III^{Glc} do not change over the pH range from 6.0 to 9.0. Given that His-75 and His-90 in III^{Glc} and His-75 in P-III^{Glc} are not cationic (Table 4), it can be concluded that the pK_a for each of these residues is less than 5.0. The fact that slight shifts are observed for the ^{15}N signals of His-90 in the unphosphorylated protein at low pH further suggest that the pK_a for His-90 is higher than that for His-75. Thus, the pK_a values for the two histidines are significantly reduced compared to the value of 7.0 found for histidine in short peptides (Bundi & Wüthrich, 1979) and the value of 6.72 found for His-105, which is a solvent-exposed residue in ribonuclease (Markley and Finkenstadt, 1975). Similarly, low pK_a's have been observed for histidine residues in several proteins (Markley, 1975), including triosephosphate isomerase (Lodi & Knowles, 1991), *E. coli* β-hydroxydecanoyl thiolester dehydrase (Annand et al., 1992), and *E. coli* Enzyme-II^{mtl} (van Dijk et al., 1992). Moreover, for P-His-90, which is protonated at N$^{\delta 1}$ and phosphorylated at N$^{\epsilon 2}$, the fact that the imidazole ring ^{1}H, ^{15}N, and ^{13}C signals are invariant up to pH 9.0 indicates that the pK_a value for P-His-90 is greater than 10. This is a significant increase compared to the pK_a of 6.4 determined for the imidazolium form of L-N$^{\epsilon 2}$-phosphohistidine (Hultquist et al., 1966). As stated previously, precise determination of the pK_a's for these histidines was precluded by aggregation of III^{Glc} and P-III^{Glc} at low pH and inefficient regeneration of the phosphorylated protein at high pH.

Factors proposed to lower the pK_a values of histidine residues in proteins include hydrogen bonding, positioning of the imidazole ring at the N-terminus of an α-helix (Hol, 1985; Perutz et al., 1985; Sali et al., 1988; Lodi & Knowles, 1991), interaction of the histidine ring with positively charged residues (Markley, 1975; Tanokura, 1983; van Dijk et al., 1990), and inclusion of the ring in a hydrophobic environment (Ikeda-Saito et al., 1977). For III^{Glc} and P-III^{Glc} a probable factor in influencing the low pK_a's of these active-site histidines relates to the fact that both His-75 and His-90 are surrounded by a ring of hydrophobic residues (Liao et al., 1991; Worthylake et al., 1991). Thus, for the unphosphorylated protein we would expect that protonation of either histidine ring would be energetically unfavorable. In this regard, Dao-pin et al. (1991) have recently shown that the apparent pK_a value of a lysine residue is lowered significantly when placed in a hydrophobic environment.

Although the structures of the active sites of III^{Glc} and P-III^{Glc} are now well characterized, questions remain concerning the mechanisms of phosphoryl transfer and signal transduction and, in particular, the role of His-75 in these processes. That His-75 is important for the full function of III^{Glc} was shown through mutagenesis studies in which His-75 and His-90 were alternately replaced with glutamine (Presper et al., 1989). In particular, the H75Q mutant was able to accept a phosphoryl group from HPr

but then was unable to donate it to the sugar. In light of this result it was suggested that the pathway for phosphoryl transfer included migration of the phosphoryl moiety from His-90 N$^{\epsilon 2}$ to His-75 N$^{\epsilon 2}$. We have shown that a proton is attached to N$^{\epsilon 2}$ of His-75 in P-III^{Glc} and that this N-H group acts as a hydrogen-bond donor with the phosphoryl oxygen atoms (Fig. 6B; Table 4). Thus, any mechanism that involves phosphoryl migration between the N$^{\epsilon 2}$ atoms of His-75 and His-90 must begin with deprotonation of His-75.

Liao et al. (1991) have suggested an alternative role for His-75. In this model His-75 N$^{\delta 1}$ becomes protonated (positively charged) upon formation of the complex between III^{Glc} and the membrane-associated protein responsible for sugar transport (IIB^{Glc}). We have shown that His-75 in uncomplexed P-III^{Glc} is neutral. Furthermore, the apparent pK_a value of His-75 in P-III^{Glc} is abnormally low (<5), indicating that protonation is energetically unfavorable. In fact, the P-His-90 moiety, which presumably carries a net charge of −1, does not induce His-75 to become protonated (positively charged). Thus, any proposal for phosphoryl transfer between P-III^{Glc} and EIIB^{Glc} that assumes protonation of His-75 must account for this barrier to protonation of the ring, for example through a conformational change at the active site and/or the close proximity of a negative charge upon complex formation.

Materials and methods

III^{Glc}$_{slow}$ was overexpressed using *E. coli* strain BL21 (DE3) (Studier & Moffatt, 1986) that had been transformed with an expression plasmid bearing the gene (*crr*) encoding for III^{Glc}. The cells were grown as described (Meadow & Roseman, 1982; Pelton et al., 1991b) using the minimal medium of Neidhardt et al. (1974) supplemented with 0.2% glucose, 2 mg/mL thiamine, and 50 mg/mL ampicillin. Protein uniformly enriched with ^{15}N or both ^{15}N and ^{13}C were obtained by growing bacteria on ^{15}NH$_4$Cl or both ^{15}NH$_4$Cl and [^{13}C$_6$]-glucose, respectively. Approximately 40 mg of ^{15}N-enriched protein, and 50 mg of uniformly ^{15}N/^{13}C-enriched protein were obtained. The ^{15}N- and ^{15}N/^{13}C-enriched samples will hereafter be denoted III^{Glc}N and III^{Glc}NC, respectively. The purity of each sample was greater than 97% based on SDS-PAGE followed by quantitative densitometric scanning of the Coomassie blue-stained gel. Enzyme I and HPr were obtained from *Salmonella typhimurium* as described (Beneski et al., 1982; Weigel et al., 1982).

Before NMR data collection on samples in H$_2$O, approximately 16 mg of III^{Glc} was dissolved in 450 μL of a 90%/10% (v/v) H$_2$O/D$_2$O solution containing 0.15 M KCl and 10 mM potassium phosphate (pH 6.4). For spectra of samples in D$_2$O, the amide protons were exchanged for deuterons by heating the protein sample for approximately 6 h at 60 °C, after which the sample was

repeatedly lyophilized from D_2O. The sample was then redissolved in D_2O, lyophilized, and finally dissolved in 450 μL of D_2O (99.998%; Cambridge Isotopes, Woburn, Massachusetts). To study the pH dependence of the NMR signals, the pH of the sample was adjusted by adding small aliquots of aqueous potassium hydroxide or HCl. Meter readings were not corrected for deuterium isotope effects.

The relatively short half-life (1.5 h) for hydrolysis of P-III^Glc at pH 6.4 (Meadow & Roseman, 1982) necessitated the use of a regeneration system (Waygood et al., 1979) that included PEP (50 mM, pH 6.4) (Sigma, St. Louis, Missouri), $MgCl_2$ (1 mM), DTT (1 mM), potassium phosphate (10 mM, pH 6.4), 0.15 M KCl, and catalytic quantities of both HPr (1.6 μM), and Enzyme I (5 units), as described (Pelton et al. 1992). Throughout the period of data collection, the extent of phosphorylation was determined by monitoring the intensity of the $H^{\varepsilon 2}$ proton of His-90 in either ^1H-^{13}C-HMQC or ^1H-^{15}N-HMQC spectra. The $H^{\varepsilon 2}$ signal was assigned previously to 7.78 ppm (III^Glc) and 8.48 ppm (P-III^Glc) on the basis of ^1H-^{15}N NOESY-HMQC spectra of the two forms of the protein (Pelton et al., 1992) and X-ray data of the unphosphorylated protein (Worthylake et al., 1991) (see below).

NMR spectroscopy

All NMR experiments except the 2D ^{13}C CCH-COSY experiment were acquired on a Bruker AMX-500 spectrometer at 36.5 °C unless noted otherwise. The 2D ^{13}C CCH-COSY experiment was acquired on a modified Bruker AM-500 spectrometer at 36.5 °C. For the HMQC-type experiments, ^1H decoupling was achieved with a 180° pulse in the middle of the t_1 time period (Bax et al., 1990c) and either ^{15}N or ^{13}C decoupling was achieved during acquisition through GARP (Shaka et al., 1985) modulation of a 2-kHz-rf field (^{15}N) or a 3.8-kHz-rf field (^{13}C).

Two-dimensional ^1H-^{15}N HMQC spectra (Bax et al., 1990c) of III^GlcN and P-III^GlcN were acquired in D_2O at pH values ranging from 6.03 to 9.11 for III^GlcN and from 6.26 to 9.05 for P-III^GlcN. The delay during which ^{15}N and ^1H signals become antiphase was set to 22 ms to refocus magnetization arising from $^1J_{NH}$ couplings. The ^1H transmitter was set to 4.67 ppm, and the ^{15}N carrier was set to 205 ppm. A total of 64 scans were signal averaged for each of 64 or 128 complex t_1 points. Acquisition times were 85.1 ms (512 complex t_2 points) and either 11.5 ms (64 complex t_1 points) or 23.0 ms (128 complex t_1 points). The States-TPPI method (Marion et al., 1989) was used to achieve quadrature detection in t_1. Note that HMBC spectra (Bax et al., 1988) are also appropriate to collect these data.

Two-dimensional ^1H-^{15}N HMQC spectra of III^GlcN and P-III^GlcN were acquired in H_2O with a 1-1 echo sup-

pression sequence (Bax et al., 1990c) at temperatures ranging from 9 to 36 °C and at pH values ranging from 6.03 to 8.58. The delay during which ^{15}N and ^1H signals become antiphase was set to 4.5 ms, slightly less than $(1/2(^1J_{NH}))$. The excitation maximum was set to 16 ppm with the ^1H transmitter set to 4.67 ppm and the ^{15}N transmitter set to 180 ppm. A total of 64 scans (512 complex points) were signal averaged for each of 128 complex t_1 points using the States-TPPI method (Marion et al., 1989) of quadrature detection in t_1. Acquisition times were 33.8 and 15.8 ms for the t_2 and the t_1 time periods, respectively.

Two-dimensional ^1H-^{13}C HMQC spectra (Bax et al., 1990c) of III^GlcNC and P-III^GlcNC were acquired at pH values ranging from 6.22 to 9.11 (III^GlcNC) and from 6.26 to 9.06 (P-III^GlcNC). The delay during which ^{13}C and ^1H signals become antiphase was set to 7.14 ms in order to attenuate phenylalanine aromatic signals ($^1J_{CH}$ ~155 Hz) relative to those of histidine ($^1J_{CH}$ 220–180 Hz) (Bystrov, 1976). The ^1H transmitter was set to 4.67 ppm, and the ^{13}C transmitter was set to 125 ppm. A total of 32 scans were signal averaged for each of 128 or 256 complex t_1 points using the States-TPPI method (Marion et al., 1989). Acquisition times were 92.1 ms (512 complex t_2 points) and either 10.2 ms (128 complex t_1 points) or 20.4 ms (256 complex t_1 points). In addition, $^1J_{CH}$ coupling constants were measured in spectra acquired with the antiphase delay set to 2.3 ms and without composite pulse decoupling.

A 2D ^{13}C CCH-COSY experiment was recorded on III^GlcNC at pH 7.50. The pulse sequence is based on the previously reported 3D HCCH-COSY experiment (Bax et al., 1990a; Kay et al., 1990). The pulse sequence used was as follows: $(90°, ^{13}C)_{\psi 1} - t_1/2 - (180°, ^1H)_{\phi 1} - t_1/2 - (90°, ^{13}C)_{\phi 2} - \Delta + \delta - (180°, ^{13}C)_x - \Delta - (180°, ^1H)_x - \delta - (90°, ^1H)_{\phi 3}(90°, ^{13}C)_x - \tau - (180°, ^1H)_x(180°, ^{13}C)_{\phi 4} - \tau - Acq_{(\phi 5)}$, with phase cycling: $\psi 1 = (x, -x)$; $\phi 1 = 2(x)$, $2(y)$, $2(-x)$, $2(-y)$; $\phi 2 = 2(x)$, $2(-x)$; $\phi 3 = 4(x)$, $4(-x)$; $\phi 4 = 2(x)$, $2(-x)$; $\phi 5 = 2(x, -x)$, $2(-x, x)$. Quadrature detection was achieved in t_1, by incrementing the phase $\psi 1$ by 90° for each t_1 point using TPPI (Marion & Wüthrich, 1983). The delays Δ, δ, and τ were set to 1.5 ms, 1.0 ms, and 1.5 ms, respectively, and the recycle delay between experiments was set to 1.0 s. The $180°_x$ ^{13}C pulse between the delays $\Delta + \delta$ and Δ was implemented as a composite pulse. The ^1H carrier was set to 4.67 ppm, and the ^{13}C carrier was set to 85 ppm. GARP modulation (Shaka et al., 1985) of a 4-kHz-rf field was used for ^{13}C decoupling during the acquisition period. A total of 512 scans were signal averaged for each of 512 (real) t_1 points. Acquisition times were 12.2 ms (t_1) and 63.5 ms (t_2) (512 complex points).

Commercial (NMRi, Syracuse, New York) and in-house software (Garrett et al., 1991) were used to process the various 2D spectra. The ^1H-^{15}N HMQC and ^1H-^{13}C HMQC data sets were processed with a Lorentzian-to-Gaussian

filter in t_1 and t_2, whereas the 2D ^{1}H-^{13}C CCH-COSY experiment was processed with a Lorentzian-to-Gaussian filter in t_2 and an unshifted sinebell filter in t_1. Each data set was zero-filled to 1K points in each dimension prior to Fourier transformation. The resulting digital resolution in the various experiments was 5.9 Hz (F_2) and 5.4 Hz (F_1) for ^{1}H-^{15}N HMQC spectra, 14.8 Hz (F_2) and 7.9 Hz (F_1) for ^{1}H-^{15}N HMQC 1-1 echo spectra, 5.4 Hz (F_2) and 12.3 Hz (F_1) for ^{1}H-^{13}C HMQC spectra, and 7.9 Hz (F_2) and 20.4 Hz (F_1) for ^{1}H-^{13}C CCH-COSY spectra. For measurement of $^1J_{CH}$ coupling constants in ^{1}H-^{13}C HMQC spectra, the data were zero-filled to 4K points in the F_2 dimension before Fourier transformation. The resulting digital resolution was 1.4 Hz/point. Chemical shifts are referenced to H_2O (4.67 ppm, 36.5 °C), external liquid ammonia (^{15}N), and sodium 3-[2,2,3,3-^{2}H$_4$]trimethyl-silylpropionate (^{13}C) (Live et al., 1984). Uncertainties in chemical shifts are 0.02 and 0.1 ppm for ^{1}H and hetero-nuclei, respectively. Uncertainties in $^1J_{CH}$ coupling constants are ±3 Hz.

Supplementary material available

Results showing ^{1}H, ^{15}N, and ^{13}C signals measured at various pH values (three figures) and ^{1}H-^{15}N HMQC exchange spectra of III^{Glc} and P-III^{Glc} collected specific periods after addition of D_2O (four figures) may be obtained from the authors.

Acknowledgments

References

Annand, R.R., Kozlowski, J.F., Davisson, V.J., & Schwab, J.M. (1993). Mechanism-based inactivation of *Escherichia coli* β-hydroxydecanoyl thiolester dehydrase: Assignment of the imidazole ^{15}N NMR resonances and determination of the structure of the alkylated histidine. *J. Am. Chem. Soc. 115*, 1088-1094.

Bachovchin, W.W. (1986). ^{15}N NMR spectroscopy of hydrogen-bonding interactions in the active site of serine proteases: Evidence for a moving histidine mechanism. *Biochemistry 25*, 7751-7759.

Bachovchin, W.W. & Roberts, J.D. (1978). Nitrogen-15 NMR Spectroscopy. The state of histidine in the catalytic triad of α-lytic protease. Implications for the charge-relay mechanism of peptide-bond cleavage by serine proteases. *J. Am. Chem. Soc. 100*, 8041-8047.

Bax, A., Clore, G.M., Driscoll, P.C., Gronenborn, A.M., Ikura, M., & Kay, L.E. (1990a). Practical aspects of proton-carbon-carbon-proton three-dimensional correlation spectroscopy of ^{13}C-labeled proteins. *J. Magn. Reson. 87*, 620-627.

Bax, A., Clore, G.M., & Gronenborn, A.M. (1990b). ^{1}H-^{1}H Correla-

tion via isotropic mixing of ^{13}C magnetization, a new three-dimensional approach for assigning ^{1}H and ^{13}C spectra of ^{13}C-enriched proteins. *J. Magn. Reson. 88*, 425-431.

Bax, A., Ikura, M., Kay, L.E., Torchia, D.A., & Tschudin, R. (1990c). Comparison of different modes of two-dimensional reverse-correlation NMR for the study of proteins. *J. Magn. Reson. 86*, 304-318.

Bax, A., Sparks, S.W., & Torchia, D.A. (1988). Long-range heteronuclear correlation: A powerful tool for the NMR analysis of medium-size proteins. *J. Am. Chem. Soc. 110*, 7926-7927.

Beneski, D.A., Nakazawa, A., Weigel, N., Hartman, P.E., & Roseman, S. (1982). Sugar transport by the bacterial phosphotransferase system. Isolation and characterization of a phosphocarrier protein HPr from wild-type and mutants of *Salmonella typhimurium. J. Biol. Chem. 257*, 14492-14498.

Blomberg, F., Maurer, W., & Rüterjans, H. (1977). Nuclear magnetic resonance investigation of ^{15}N-labeled histidine in aqueous solution. *J. Am. Chem. Soc. 99*, 8149-8159.

Bundi, A., & Wüthrich, K. (1979). ^{1}H NMR parameters of the common amino acid residues measured in aqueous solutions of the linear tetrapeptides H-GLY-GLY-X-L-ALA-OH. *Biopolymers 18*, 285-297.

Bystrov, V.F. (1976). Spin-spin coupling and the conformational states of peptide systems. *Prog. NMR Spectrosc. 10*, 41-81.

Clore, G.M., Bax, A., Driscoll, P.C., Wingfield, P.T., & Gronenborn, A.M. (1990). Assignment of the side-chain ^{1}H and ^{13}C resonances of interleukin-1β using double and triple resonance heteronuclear 3D NMR spectroscopy. *Biochemistry 29*, 8172-8184.

Clore, M.G. & Gronenborn, A.M. (1991). Structures of larger proteins in solution: Three- and four-dimensional heteronuclear NMR spectroscopy. *Science 252*, 1390-1399.

Dao-pin, S., Anderson, D.E., Baase, W.A., Dahlquist, F.W., & Matthews, B.W. (1991). Structural and thermodynamic consequences of burying a charged residue within the hydrophobic core of T4 lysozyme. *Biochemistry 30*, 11521-11529.

Dörschug, M., Frank, R., Kalbitzer, R.H., Hengstenberg, W., & Deutscher, J. (1984). Phosphoenolpyruvate-dependent phosphorylation site in Enzyme III^{Glc} of the *Escherichia coli* phosphotransferase system. *Eur. J. Biochem. 144*, 113-119.

El Kabbani, O.A.L., Waygood, E.B., & Delbaere, L.T.J. (1987). Tertiary structure of the histidine containing protein of the phosphoenolpyruvate:sugar phosphotransferase system of *Escherichia coli. J. Biol. Chem. 262*, 12926-12929.

Fairbrother, W.J., Cavanagh, J., Dyson, H.J., Palmer, A.G., III, Sutrina, S.L., Reizer, J., Saier, M.H., Jr., & Wright, P.E. (1991a). Polypeptide backbone resonance assignments and secondary structure of *Bacillus subtilis* Enzyme III^{Glc} determined by two-dimensional and three-dimensional heteronuclear NMR spectroscopy. *Biochemistry 30*, 6896-6907.

Fairbrother, W.J., Gippert, G.P., Reizer, J., Saier, M.H., & Wright, P.E. (1991b). Low resolution solution structure of the *Bacillus subtilis* glucose permease IIA domain derived from heteronuclear three-dimensional NMR spectroscopy. *FEBS. Lett. 296*, 148-152.

Fairbrother, W.J., Palmer, A.G., III, Rance, M., Reizer, J., Saier, M.H., Jr., & Wright, P.E. (1992). Assignment of the aliphatic ^{1}H and ^{13}C resonances of the *Bacillus subtilis* glucose permease IIA domain using double- and triple-resonance heteronuclear three-dimensional NMR spectroscopy. *Biochemistry 31*, 4413-4425.

Fesik, S.W. & Zuiderweg, E.R.P. (1990). Heteronuclear three-dimensional NMR spectroscopy of isotopically labelled biological macromolecules. *Q. Rev. Biophys. 23*, 97-131.

Garrett, D.S., Powers, R., Gronenborn, A.M., & Clore, G.M. (1991). A common sense approach to peak picking in two-, three-, and four-dimensional spectra using automatic computer analysis of contour diagrams. *J. Magn. Reson. 95*, 214-220.

Grzesiek, S. & Bax, A. (1992). An efficient experiment for sequential assignment of medium sized isotopically enriched proteins. *J. Magn. Reson. 99*, 201-207.

Harbison, G., Herzfeld, J., & Griffin, R.G. (1981). Nitrogen-15 chemical shift tensors in L-histidine hydrochloride monohydrate. *J. Am. Chem. Soc. 103*, 4752-4754.

Hammen, P.K., Waygood, E.B., & Klevit, R. (1991). Reexamination of the secondary and tertiary structure of histidine-containing protein from *Escherichia coli* by homonuclear and heteronuclear NMR spectroscopy. *Biochemistry 30*, 11842-11850.

Hansen, P.E. (1983). Isotope effects on nuclear shielding. *Annu. Rep. NMR Spectrosc. 15*, 174.

Herzberg, O., Reddy, P., Sutrina, S., Saier, M.H., Jr., Reizer, J., & Kapadia, G. (1992). Structure of the histidine-containing phosphocarrier protein HPr from *Bacillus subtilis* at 2.0-Å resolution. *Proc. Natl. Acad. Sci. USA 89*, 2499–2503.

Hol, W.G.J. (1985). The role of the α-helix dipole in protein function and structure. *Prog. Biophys. Mol. Biol. 45*, 149–195.

Howarth, O.W. & Lilley, D.M. (1978). Carbon-13 NMR of peptides. *Progr. NMR Spectrosc. 12*, 1–40.

Hultquist, D.E., Moyer, R.W., & Boyer, P.D. (1966). The preparation and characterization of 1-phosphohistidine and 3-phosphohistidine. *Biochemistry 5*, 322–331.

Ikeda-Saito, M., Iizuka, T., Yamamoto, H., Kayne, F.J., & Yonetani, T. (1977). Studies on cobalt myoglobins and hemoglobins. Interaction of sperm whale myoglobin and glycern hemoglobin with molecular oxygen. *J. Biol. Chem. 252*, 4882–4887.

Kay, L.E., Ikura, M., & Bax, A. (1990). Proton–proton correlation via carbon–carbon couplings: A three-dimensional NMR approach for the assignment of aliphatic resonances in proteins labeled with ^{13}C. *J. Am. Chem. Soc. 112*, 888–889.

Klevit, R.E. & Waygood, E.B. (1986). Two-dimensional ^{1}H NMR studies of histidine-containing protein from *Escherichia coli*, 3. Secondary and tertiary structure as determined by NMR. *Biochemistry 25*, 7774–7781.

Liao, D.-I., Kapadia, G., Reddy, P., Saier, M.H., Jr., Reizer, J., & Herzberg, O. (1991). Structure of the IIA domain of the glucose permease of *Bacillus subtilis* at 2.2 Å resolution. *Biochemistry 30*, 9583–9594.

Live, D.H., Davis, D.G., Agosta, W.C., & Cowburn, D. (1984). Long range hydrogen bond mediated effects in peptides: ^{15}N NMR study of gramicidin S in water and organic solvents. *J. Am. Chem. Soc. 106*, 1939–1941.

Lodi, P.J. & Knowles, J.R. (1991). Neutral imidazole is the electrophile in the reaction catalyzed by triosephosphate isomerase: Structural origins and catalytic implications. *Biochemistry 30*, 6948–6956.

Marion, D., Ikura, M., Tschudin, R., & Bax, A. (1989). Rapid recording of 2D NMR spectra without phase cycling. Application to the study of hydrogen exchange in proteins. *J. Magn. Reson. 85*, 393–399.

Marion, D. & Wüthrich, K. (1983). Application of phase sensitive two-dimensional correlated spectroscopy (COSY) for measurement of ^{1}H-^{1}H spin-spin couplings in proteins. *Biochem. Biophys. Res. Commun. 113*, 967–974.

Markley, J.L. (1975). Observation of histidine residues in proteins by means of NMR spectroscopy. *Acc. Chem. Res. 8*, 70–80.

Markley, J.L. & Finkenstadt, W.R. (1975). Correlation proton magnetic resonance studies at 250 MHz of bovine pancreatic ribonuclease. III. Mutual electrostatic interaction between histidine residues 12 and 119. *Biochemistry 14*, 3562–3566.

Meadow, N.D., Fox, D.K., & Roseman, S. (1990). The bacterial phosphoenolpyruvate:glycose phosphotransferase system. *Annu. Rev. Biochem. 59*, 497–542.

Meadow, N.D. & Roseman, S. (1982). Sugar transport by the bacterial phosphotransferase system. Isolation and characterization of a glucose specific phosphocarrier protein (III^{Glc}) from *Salmonella typhimurium*. *J. Biol. Chem. 257*, 14526–14537.

Munowitz, M., Bachovchin, W.W., Herzfeld, J., Dobson, C.M., & Griffin, R.G. (1982). Acid–base and tautomeric equilibria in the solid-state: ^{15}N NMR spectroscopy of histidine and imidazole. *J. Am. Chem. Soc. 104*, 1192–1196.

Neidhardt, F.C., Block, P.L., & Smith, D.F. (1974). Culture medium for enterobacteria. *J. Bacteriol. 119*, 736–747.

Pelton, J.G., Torchia, D.A., Meadow, N.D., & Roseman, S. (1992). Structural comparison of phosphorylated and unphosphorylated forms of III^{Glc}, a signal-transducing protein from *Escherichia coli*, using three-dimensional NMR techniques. *Biochemistry 31*, 5215–5224.

Pelton, J.G., Torchia, D.A., Meadow, N.D., Wong, C.-Y., & Roseman, S. (1991a). Secondary structure of the phosphocarrier protein III^{Glc}, a signal-transducing protein from *Escherichia coli*, determined by heteronuclear three-dimensional NMR spectroscopy. *Proc. Natl. Acad. Sci. USA 88*, 3479–3488.

Pelton, J.G., Torchia, D.A., Meadow, N.D., Wong, C.-Y., & Roseman,

S. (1991b). ^{1}H, ^{15}N, and ^{13}C NMR signal assignments of III^{Glc}, a signal-transducing protein of *Escherichia coli*, using three-dimensional triple-resonance techniques. *Biochemistry 30*, 10043–10057.

Perutz, M.F., Gronenborn, A.M., Clore, G.M., Fogg, J.H., & Shih, D.T.-b. (1985). The pK_a values of two histidine residues in human haemoglobin, the Bohr effect, and the dipole moments of α-helices. *J. Mol. Biol. 183*, 491–498.

Postma, P.W. & Lengeler, J. (1985). Phosphoenolpyruvate:carbohydrate phosphotransferase system of bacteria. *Microbiol. Rev. 49*, 232–269.

Presper, K.A., Wong, C.-Y., Liu, L., Meadow, N.D., & Roseman, S. (1989). Site-directed mutagenesis of the phosphocarrier protein, III^{Glc}, a major signal-transducing protein in *Escherichia coli*. *Proc. Natl. Acad. Sci. USA 86*, 4052–4055.

Redfield, A.G. & Papastavros, M.Z. (1990). NMR study of the phosphoryl binding loop in purine nucleotide proteins: Evidence for strong hydrogen bonding in human N-ras-p21. *Biochemistry 29*, 3509–3514.

Reynolds, W.F., Peat, I.R., Freedman, M.H., & Lyerla, J.R., Jr. (1973). Determination of the tautomeric form of the imidazole ring of L-histidine in basic solution by carbon-13 magnetic resonance spectroscopy. *J. Am. Chem. Soc. 95*, 338–331.

Richarz, R. & Wüthrich, K. (1978). Carbon-13 NMR chemical shifts of the common amino acid residues measured in aqueous solutions of the linear tetrapeptides H-Gly-Gly-X-L-ALA-OH. *Biopolymers 17*, 2133–2141.

Roberts, J.D., Yu, C., Flanagan, C., & Birdseye, T.R. (1982). A nitrogen-15 NMR study of acid–base and tautomeric equilibria of 4-substituted imidazoles and its relevance to the catalytic mechanism of α-lytic protease. *J. Am. Chem. Soc. 104*, 3945–3949.

Roseman, S. & Meadow, N.D. (1990). Signal transduction by the bacterial phosphotransferase system, diauxie, and the *crr* gene. *J. Biol. Chem. 265*, 2993–2996.

Saier, M.H., Jr. (1989). Protein phosphorylation and allosteric control of inducer exclusion and catabolite repression by the bacterial phosphoenolpyruvate:sugar phosphotransferase system. *Microbiol. Rev. 53*, 109–120.

Sali, D., Bycroft, M., & Fersht, A.R. (1988). Stabilization of protein structure by interaction of a α-helix dipole with a charged sidechain. *Nature 335*, 740–743.

Schuster, I.I. & Roberts, J.D. (1979). Nitrogen-15 NMR spectroscopy. Effects of hydrogen bonding and protonation on nitrogen chemical shifts in imidazoles. *J. Org. Chem. 44*, 3864–3867.

Shaka, A.J., Barker, P., & Freeman, R. (1985). Computer-optimized decoupling scheme for wideband applications and low level operation. *J. Magn. Reson. 64*, 547–552.

Sharma, S., Georges, F., Delbaere, L.T.J., Lee, J.S., Klevit, R.E., & Waygood, E.B. (1991). Epitope mapping by mutagenesis distinguishes between the two tertiary structures of the histidine containing protein HPr. *Proc. Natl. Acad. Sci. USA 88*, 4877–4881.

Stothers, J.B. (1972). *Carbon-13 NMR Spectroscopy*. Academic Press, New York.

Studier, F.W. & Moffatt, B.A. (1986). Use of bacteriophage T7 RNA polymerase to direct selective high level expression of cloned genes. *J. Mol. Biol. 189*, 113–130.

Tanokura, M. (1983). ^{1}H-NMR study of the tautomerism of the imidazole ring of histidine residues. *Biochim. Biophys. Acta 742*, 586–596.

Tran-Dinh, S., Fermandhan, S., Sala, E., Mermet-Bouvier, R., Cohen, M., & Fromageot, P. (1975). Geminal and vicinal ^{13}C-^{13}C coupling constants of 85% ^{13}C-enriched amino acids. *J. Am. Chem. Soc. 97*, 1267–1268.

van Dijk, A.A., de Lange, L.C.M., Bachovchin, W.W., & Robillard, G.T. (1990). Effect of phosphorylation on hydrogen-bonding interactions of the active site histidine of HPr determined by ^{15}N NMR spectroscopy. *Biochemistry 29*, 8164–8171.

van Dijk, A.A., Scheek, R.M., Dijkstra, K., Wolters, G.K., & Robillard, G.T. (1992). Characterization of the protonation and hydrogen bonding state of the histidine residues in IIA^{mtl}, a domain of the phosphoenolpyruvate-dependent mannitol-specific transport protein. *Biochemistry 31*, 9063–9072.

van Nuland, N.A.J., van Dijk, A.A., Dijkstra, K., van Hoesel, F.H.J., Scheck, R.D., & Robillard, G.T. (1992). Three-dimensional nitrogen-15-proton-proton and nitrogen-15-carbon-13-proton nuclear magnetic resonance studies of HPr, a central component of the phos-

phoenolpyruvate-dependent phosphotransferase system from *Escherichia coli*. Assignment of backbone resonances. *Eur. J. Biochem.* 203, 483–491.

Wagner, G., Pardi, A., & Wüthrich, K. (1983). Hydrogen bond lengths and ^{1}H NMR chemical shifts in proteins. *J. Am. Chem. Soc.* 105, 5948–5949.

Walters, D.E. & Allerhand, A. (1980). Tautomeric states of the histidine residues of bovine pancreatic ribonuclease A. *J. Biol. Chem.* 255, 6200–6204.

Wang, J., Hinck, A.P., Loh, S.N., & Markley, J.L. (1990). Two-dimensional NMR studies of staphylococcal nuclease: III. Evidence for conformational heterogeneity from ^{1}H, ^{13}C and ^{15}N spin system assignments of the aromatic amino acids in the nuclease H124L–thymidine-3',5'-bisphosphate–Ca^{2+} ternary complex. *Biochemistry 29*, 102–113.

Waygood, E.B., Meadow, N.D., & Roseman, S. (1979). Modified assay procedures for the phosphotransferase system in enteric bacteria. *Anal. Biochem.* 95, 293–304.

Weigel, N., Waygood, E.B., Kukuruzinska, M.A., Nakazawa, A., & Roseman, S. (1982). Sugar transport by the bacterial phosphotransferase system. Isolation and characterization of Enzyme I from *Salmonella typhimurium*. *J. Biol. Chem.* 257, 14461–14469.

Witanowski, M., Stefaniak, L., Januszewski, H., Grabowski, Z., & Webb, G.A. (1972). Nitrogen-14 nuclear magnetic resonance of azoles and their benzo derivatives. *Tetrahedron 28*, 637–653.

Witanowski, M., Stefaniak, L., & Webb, G.A. (1986). Nitrogen NMR spectroscopy. *Annu. Rep. NMR Spectrosc. 18*, 1–763.

Wittekind, M.G., Rajagopal, P., Reizer, J., & Klevit, R.E. (1992). Solution structure of the histidine-containing protein from *Bacillis subtilis*. *Protein Sci. 1*, 1363–1376.

Worthylake, D., Meadow, N.D., Roseman, R., Liao, D.-I., Herzberg, O., & Remington, S.J. (1991). Three-dimensional structure of the *Escherichia coli* phosphocarrier protein III^{Glc}. *Proc. Natl. Acad. Sci USA 88*, 10382–10386.

Wüthrich, K. (1986). *NMR of Proteins and Nucleic Acids*. Wiley, New York.